Soft Switching Boost converter using a Passive LC Resonating Network

Name of the author	Affiliation	Address
ARKAPRIO BHATTACHARYA	Student, JIS College of Engineering	Konnagar, Hooghly, West Bengal
DHURJATI PROLOY BISWAS	Student, JIS College of Engineering	Barasat, 24 Parganas(N), West Bengal
DISHA DEBNATH	Student, JIS College of Engineering	Dinhata, Cooch Behar, West Bengal
RUPAM SAHA	Student, JIS College of Engineering	Bangaon, 24 Parganas(N), West Bengal
SATTICK CHANDA	Student, JIS College of Engineering	Baranagar, 24 Parganas(N), West Bengal
SAYANTAN ROY	Student, JIS College of Engineering	Kanchrapara, 24 Parganas(N), West Bengal
SOHOM SAHA	Student, JIS College of Engineering	Pandua, Hooghly, West Bengal
UDAYAN KUMAR NATH	Student, JIS College of Engineering	Bandel, Hooghly, West Bengal
BISWAMOY PAL	Asst. Professor, JIS College of Engineering	Kalyani, Nadia, West Bengal

Abstract:

A soft-switching boost converter utilizing a passive LC resonant network is designed, simulated, and implemented in this paper. Traditional boost converter implements hard switching methods which leads to high switching loss. This makes it viable for low frequency applications, leading to poor power density. This limits them in high frequency as loss reaches very high level. The primary objective of this work is to mitigate switching losses, enabling high frequency operation with improved power density and efficiency. Theoretical concepts, design process and simulation results validation of the proposed converter is described.

Introduction:

In recent years, the demand for electricity generation systems based on nonconventional energy sources has driven the development of a new generation of high-gain DC-DC converters [1]. These high-gain converters can be categorized as either isolated or non-isolated. Among them, transformer less (non-isolated) topologies have gained popularity in medium-power applications (up to 400–500 W) due to their cost-effectiveness and high efficiency. Traditional DC-DC converter topologies such as boost, SEPIC, and ZETA offer simple structures but suffer from low efficiency. Achieving a high voltage gain with these topologies requires operating at high duty cycles, which leads to increase stress on switching components. To address these challenges, a variety of high-gain DC-DC converter topologies have been developed. Each configuration has its own advantages and disadvantages. Techniques like switched capacitors, voltage multiplier cells (VMCs) and switched inductors are commonly used to enhance the voltage gain. While isolated converters offer advantages like common ground, isolation and high efficiency—ideal for high-power applications—non-isolated high-gain converters are also suitable for microgrid systems with bidirectional power flow [3]. A non-isolated, switched-capacitor-based boost converter using two inductors and a single switch was introduced in [4], though its voltage gain was limited. In photovoltaic (PV) systems, a step-up converter is essential to increase the voltage level as part of the MPPT (Maximum Power Point Tracking) process. An improved boost converter tailored for renewable energy applications was proposed in [5], while [6,7] presented high-gain boost and SEPIC converters featuring continuous input current. Many approaches have been proposed to achieve higher gain at lower cost and better efficiency. A generalized high-gain DC-DC converter structure using a single switch and switched inductors was introduced in [8]. The quadratic boost technique has also been employed to enhance gain, albeit with high voltage stress on components [9], which necessitates the use of high-rated switches, increasing conduction losses [10]. The conventional quadratic boost converter (CQBC), as proposed in [11], also experiences a voltage stress equal to the output voltage across its single switch. In [12], a voltage doubler circuit utilizing diodes and switched capacitors was proposed to substantially boost the output voltage. Similarly, a DC-DC Luo converter delivering a positive output voltage using switched capacitors and diodes was proposed in [13]. Coupled inductor-based topologies are another popular approach for achieving high gain, but they typically result in larger input current ripples. Some of the issues related to these topologies have been addressed in the converters proposed in [14–17]. Voltage multiplier cells (VMCs) integrated with traditional converters like boost, SEPIC, and CQBC have been shown to further increase gain, as discussed in [18–20]. However, VMCs using switched capacitors often suffer from high charging currents, leading to extra power losses. Additionally, the component count increases, which in turn raises costs and reduces reliability. Interleaved boost converters form another category of high-gain converters, delivering significant gain even at lower duty cycles. However, they typically need several VMCs at the output stage [21–24]. The converter proposed in the current study stands out for its simplicity and performance. Key features include:

- Reduced electromagnetic interference.
- Improved efficiency.
- Improved power density.
- Enhanced reliability.

The detailed functioning of the proposed converter is explained in the upcoming sections.

<u>Circuit diagram:</u>

The circuit diagram of the proposed soft switched boost converter is shown in fig 1. Apart from the basic boost converter elements, the proposed converter uses only one resonating inductor (L_r) and a resonating capacitor (C_r) to achieve soft transition of the main switch both at turn on and turn off. The details of converter modes of operations at different stages are described below. The equivalent circuits in each mode and related key waveforms are depicted in fig 2 and 5 respectively.

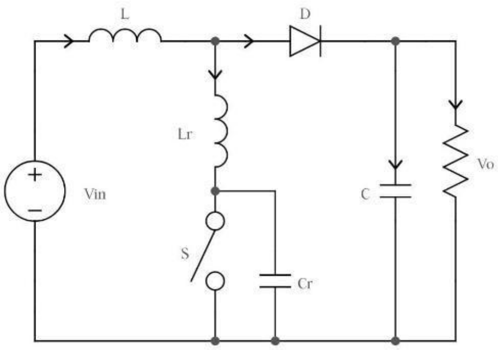

Fig.1

Traditional boost converter employees hard switching methods which leads to switching losses. This loss is miniscule for one cycle thus negligible in low frequency applications but increases exponentially and reaches high levels when implementing in high frequency applications above
20 kHz. So, to mitigate this issue the proposed converter employees soft switching methods like ZCS and ZVS which reduces the switching loss per cycle. This enables the converter to be operated in high frequency conditions without incurring significant loss and performance issues.

International Scientific Journal of Engineering and Management (ISJEM) ISSN: 2583-6129
Volume: 04 Issue: 04 | April – 2025 DOI: 10.55041/ISJEM03246
An International Scholarly || Multidisciplinary || Open Access || Indexing in all major Database & Metadata

Methods:

Let us assume that the current is flowing from the current source to the load through the diode in the outer circuit and the inner inductor (L_r) and capacitor (C_r) are fully discharged. Now the switch is just turned on and the current through the inductor (i_{Lr}) is slowly rising and it is getting charged. The whole input current is flowing through the inductor (L_r) and the diode is switched off isolating the load terminal. The inductor (L_r) is fully charged and the current (i_{Lr}) through it. The switch is just turned off and the capacitor (C_r) is getting charged with the combined current from the input and inductor (L_r) . The inductor (L_r) gets completely discharged to capacitor (C_r) and the capacitor gets charged to the point where the diode is turned on. Consequently, inductor current (i_{Lr}) becomes zero and the capacitor voltage (V_{Cr}) reaches its peak. The capacitor (C_r) is fully discharged and the inductor (L_r) is fully charged which turns on the flyback diode (D_r). So, the inductor discharges itself to the load through the flyback diode.

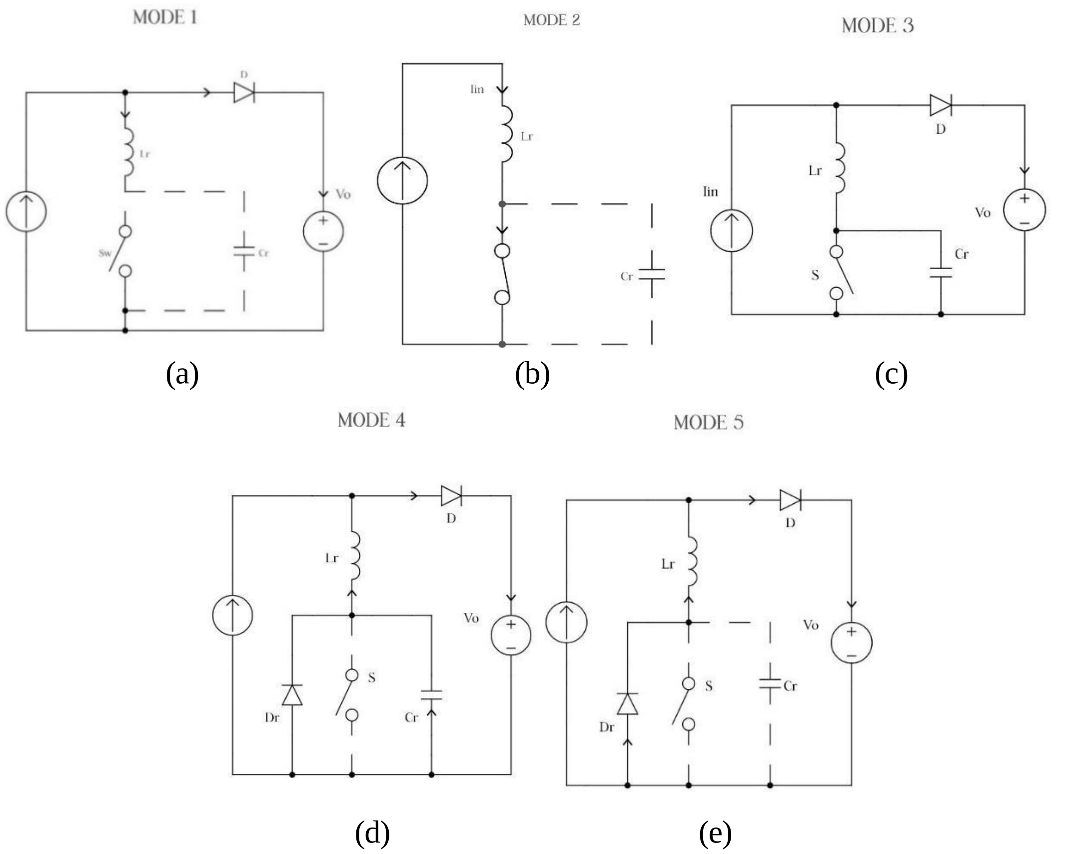

Fig.2
Equivalent circuit in each operating mode

In the given circuit, as we have a DC voltage source connected to a large inductor, we can replace them with a current source in the equivalent circuit.

Mode -1: ($t_0 - t_1$)

Let us assume that the current is flowing from the current source to the load through the diode in the outer circuit and the inner inductor (L_r) and capacitor (C_r) are fully

International Scientific Journal of Engineering and Management (ISJEM) ISSN: 2583-6129
Volume: 04 Issue: 04 | April – 2025 DOI: 10.55041/ISJEM03246
An International Scholarly || Multidisciplinary || Open Access || Indexing in all major Database & Metadata

discharged. Now the switch is just turned on and the current through the inductor (i_{Lr}) is slowly rising and it is getting charged. It is given by the equation below:

$$i_{Lr}(t) = \frac{V_0}{L_r}(t - t_0)$$

$$\text{Time duration: } \Delta t_{01} = t_1 - t_0 = \frac{I_{in} L_r}{V_0}$$

Mode- 2: ($t_1 - t_2$)

In this mode, the whole input current is flowing through the inductor (L_r) and the diode is switched off isolating the load terminal. The inductor (L_r) is fully charged and the current (i_{Lr}) through it is given by the equation below:

$$i_{Lr}(\text{t}) = I_{in}$$

$$\text{Time duration: } \Delta t_{12} = t_2 - t_1 = \text{D}T_{sw} - \Delta t_{01}$$

Mode- 3:($t_2 - t_3$)

In this mode, the switch is just turned off and the capacitor (C_r) is getting charged with the combined current from the input and inductor (L_r) simultaneously and reaches to the peak and the inductor current becomes zero. The equation is given below:

$$i_{Lr}(t) = \frac{V_0}{Z_r}\sin(\omega_r(t - t_2)) + I_{in}cos(\omega_r(t - t_2))$$

$$V_{Cr}(t) = V_0 - V_0\cos(\omega_r(t - t_0)) + I_{in}Z_r\sin(\omega_r(t - t_2))$$

$$\text{Time duration: } \Delta t_{23} = t_3 - t_2 = \frac{1}{\omega_r} tan^{-1}\left(\frac{-I_{in}Z_r}{V_0}\right)$$

The peak voltage of capacitor: V= $V_{Cr}(t_3) = V_0 - V_0\cos(\omega_r(t_3 - t_2)) + I_{in}Z_r\sin(\omega_r(t_3 - t_2))$

Mode- 4:($t_3 - t_4$)

In this mode, initially the capacitor voltage is at peak and the diode is turned on. The capacitor gets discharged and voltage (V_{Cr}) reaches zero. And the inductor current equation is given below:

$$i_{Lr}(t) = \frac{V_0 - V}{C_r}\sin(\omega_r(t - t_3))$$

$$V_{Cr}(t) = (V_0 - V)(1 - \cos(\omega_r(t - t_0)))$$

$$\text{Time duration: } \Delta t_{34} = t_4 - t_3 = \frac{1}{\omega_r} cos^{-1}\left(\frac{V_0}{V_0 - V}\right)$$

Mode- 5:($t_4 - t_5$)

At this point, the capacitor (C_r) is fully discharged and the inductor (L_r) is fully charged which turns on the flyback diode (D_r). So, the inductor discharges itself to the load through the flyback diode. And the inductor current equation is given below:

$$i_{Lr}(t) = \frac{V_0}{L_r}(t - t_4) + \frac{V_0 - V}{Z_r} sin\omega_r(t_4 - t_3)$$

$$\text{Time duration: } \Delta t_{45} = t_5 - t_4 = \frac{L_r}{Z_r}\frac{V - V_0}{Z_r}\sin\omega_r(t_4 - t_3)$$

Circuit Parameters:

Sl No.	Components	Value
1.	Input Voltage	24 V
2.	Boost Inductor	500 µH
3.	Resonant Inductor	20 µH
4.	Resonant Capacitor	400 nF
5.	Frequency	50 kHz

- **Boundary conditions: -**

For determining the boundary condition of the boost inductor for CCM and DCM, the ripple should be less than average current. If the ripple is Δi and the average current is i_{avg} then the condition for the conduction mode in CCM is,

$$\Delta i/2 < i_{avg}$$

Now, for an inductor, $V = L\frac{di}{dt}$

$$di = \frac{V}{L}DT$$

$$\therefore \Delta i = \frac{V_{in}DT}{L}$$

Therefore, from boundary condition equation,

$$\frac{V_{in}}{2L}DT < \frac{P_o}{V_{in}} \quad [\because i_{avg} = \frac{P_{in}}{V_{in}} \text{ and } P_{in} = P_o$$

$$\text{or, } \frac{V_{in}}{2L}DT < \frac{{V_o}^2}{R_o V_{in}}$$

$$\text{or, } \frac{L}{R_o T} > \frac{1}{2}\left(\frac{V_{in}}{V_o}\right)^2 D$$

$$\text{or, } \tau > \frac{1}{2}\left(\frac{V_{in}}{V_o}\right)^2 D$$

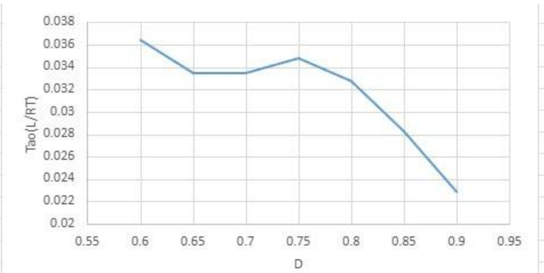

Fig.3

So, from the graph for D = 0.75, the boundary condition value for τ is around 0.03. If the resistance is 75Ω and $T = \frac{1}{50 * 10^3}$, then $L = 45 * 10^{-6}$ H. Thus, the chosen value for our boost inductor is

$L = 50 * 10^{-5}$ H.

Now, $\tau = \frac{L}{RT}$.
So, if L and T are constants then $\tau \propto \frac{1}{R}$.
And for power, $P = \frac{Vo^2}{R}$
So, if output voltage is constant then $P \propto \frac{1}{R}$.
So, $\tau \propto P$.
In other words, the system will be in CCM at 10% load condition.

- **Ripple analysis: -**

The condition of ripple for the inductor of this circuit

$$Ripple = \frac{di}{i_{avg}} * 100$$

Now, Ripple current, $di = \frac{Vin}{L} DT$ and average current, $i_{avg} = \frac{P_o}{V_{in}}$.
$\therefore$ for $V_{in} = 24\ V$, D = 0.75, $T = \frac{1}{50 * 10^3}$.

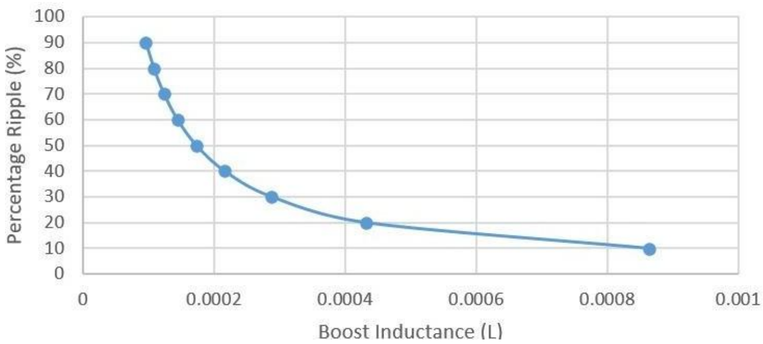

Fig.4

From the graph it can be inferred that for getting ripple less than 20%, the inductance needs to be more than 0.000432, thus our chosen inductance is $50 * 10^{-5}$ H, has the percentage ripple less than 20.

International Scientific Journal of Engineering and Management (ISJEM) ISSN: 2583-6129
Volume: 04 Issue: 04 | April – 2025 DOI: 10.55041/ISJEM03246
An International Scholarly || Multidisciplinary || Open Access || Indexing in all major Database & Metadata

Results:

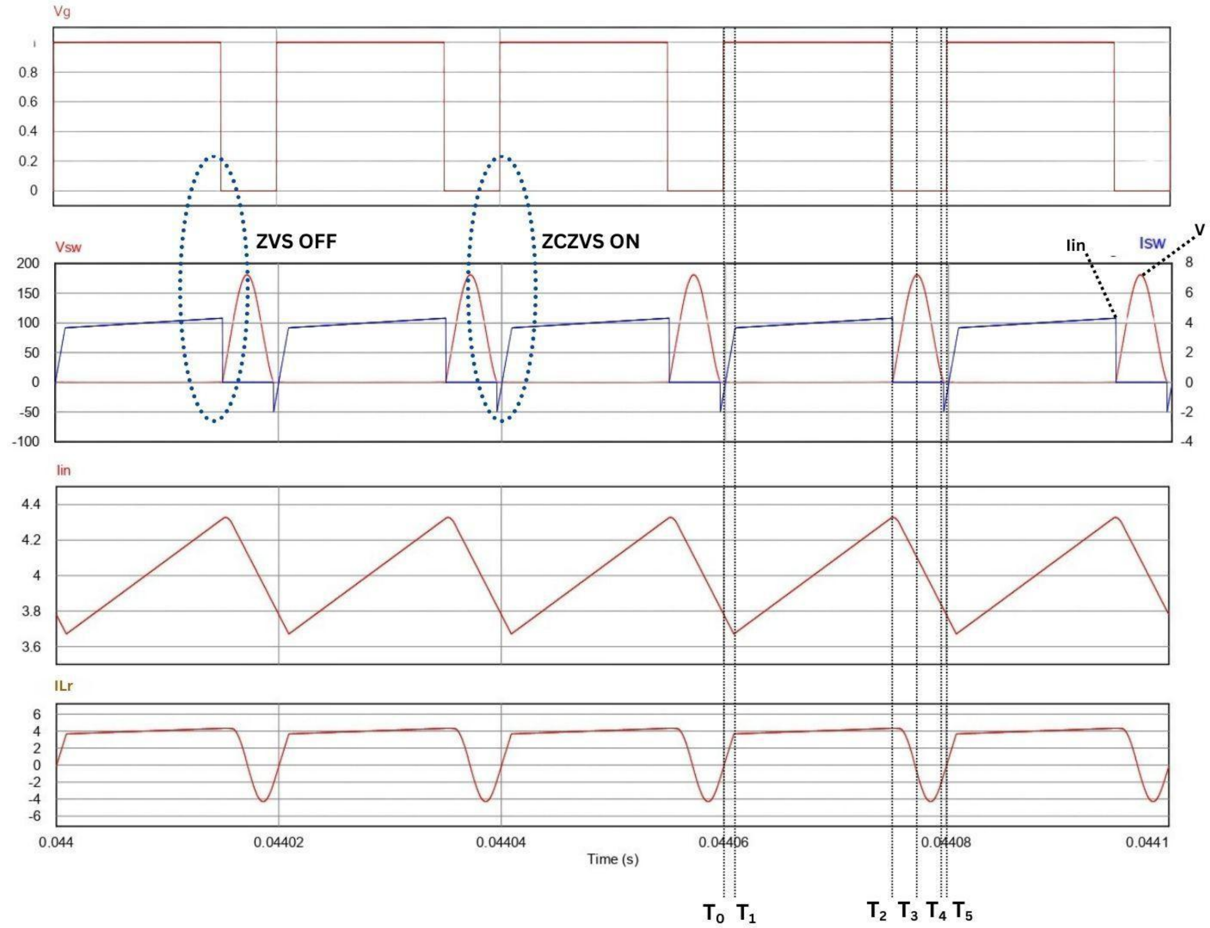

Indexing	
V_g	Gate Pulse
I_{in}	Input Current
I_{L2}	Resonating Inductor
V_{sw}	Switch Voltage
I_{sw}	Switch Current

Fig.5

ISSN: 2583-6129
DOI: 10.55041/ISJEM03246

Discussion:

From the waveform depicted in fig.5 we can observe that the proposed converter is under ZVS OFF and ZCZVS ON and thus is being successfully softswitch. This negates switching loss and enables high frequency operations. This converter current has a ripple percentage of less than 20 which makes current more stable. This converter reduces energy loss which makes it more efficient in energy management and thus reduces energy usage as a whole when implemented in practical scenarios in large scale. This ideology aligns with a global push for sustainable and green energy management through scientific progress and discoveries.

Conclusion:

A passive LC resonant network was effectively used to design and implement a soft-switching boost converter. By mitigating switching losses, the converter offers significant improvements in efficiency and power density. Future research can explore advanced control techniques and wide-bandgap devices to further enhance the performance and capabilities of such converters.

The future of soft-switching boost converters is promising, with several avenues for further research and development:

1. Integration of Wide-Bandgap Devices:

   Utilizing wide-bandgap semiconductors like Silicon Carbide (SiC) and Gallium Nitride (GaN) can further improve efficiency and power density.

   These devices offer higher switching speeds and lower conduction losses, enabling higher-frequency operation and reduced switching losses.

2. Advanced Control Techniques:

   Developing advanced control strategies, such as digital control, predictive control, and model-predictive control, can optimize the performance of soft-switching converters under various operating conditions.

   These techniques can improve efficiency, stability, and dynamic response.

3. Multiphase Converters:

   Employing multiphase configurations can further reduce current stress on individual components and improve power quality.

   These converters can also be used to achieve higher power levels and improved thermal management.

4. Integration with Renewable Energy Systems:

   Soft-switching converters can be integrated with renewable energy sources like solar and wind power to improve the efficiency and reliability of these systems.

By optimizing the power flow and energy storage, these converters can enhance the overall performance of renewable energy systems.

5. Electric Vehicle Applications:

Soft-switching converters can be used in electric vehicles to improve the efficiency and range of these vehicles. By reducing power losses and improving power density, these converters can contribute to the advancement of electric vehicle technology.

By addressing these areas, future research can lead to even more efficient, reliable, and powerful soft-switching boost converters.

References:

1. Forouzesh, M.; Siwakoti, Y.P.; Gorji, S.A.; Blaabjerg, F.; Lehman, B. Step-Up DC–DC Converters: A Comprehensive Review of Voltage-Boosting Techniques, Topologies, and Applications. *IEEE Trans. Power Electron.* **2017**, *32*, 9143–9178. [Google Scholar] [CrossRef]
2. Tofoli, F.L.; Pereira, D.D.C.; de Paula, W.J.; Júnior, D.D.S.O. Survey on non-isolated high-voltage step-up dc–dc topologies based on the boost converter. *IET Power Electron.* **2015**, *8*, 2044–2057. [Google Scholar] [CrossRef] [Green Version]
3. Cornea, O.; Andreescu, G.-D.; Muntean, N.; Hulea, D. Bidirectional Power Flow Control in a DC Microgrid Through a Switched-Capacitor Cell Hybrid DC–DC Converter. *IEEE Trans. Ind. Electron.* **2017**, *64*, 3012–3022. [Google Scholar] [CrossRef]
4. Shahir, F.M.; Babaei, E.; Farsadi, M. Voltage-Lift Technique Based Nonisolated Boost DC–DC Converter: Analysis and Design. *IEEE Trans. Power Electron.* **2017**, *33*, 5917–5926. [Google Scholar] [CrossRef]
5. Padmanaban, S.; Bhaskar, M.S.; Maroti, P.K.; Blaabjerg, F.; Fedák, V. An original transformer and switched capacitor (T & SC)- based extension for DC-DC boost converter for high-voltage/low- current renewable energy applica-tions: Hardware implementation of a new T & SC boost converter. *Energies* **2018**, *11*, 783. [Google Scholar] [CrossRef] [Green Version]
6. Saravanan, S.; Babu, N.R. Design and Development of Single Switch High Step-Up DC–DC Converter. *IEEE J. Emerg. Sel. Top. Power Electron.* **2017**, *6*, 855–863. [Google Scholar] [CrossRef]
7. Banaei, M.R.; Sani, S.G. Analysis and Implementation of a New SEPIC-Based Single-Switch Buck–Boost DC–DC Converter With Continuous Input Current. *IEEE Trans. Power Electron.* **2018**, *33*, 10317–10325. [Google Scholar] [CrossRef]
8. Shanthi, T.; Prabha, S.U.; Sundaramoorthy, K. Non-isolated n-stage High Step-up DC-DC Converter for Low voltage DC Source Integration. *IEEE Trans. Energy Convers.* **2021**. [Google Scholar] [CrossRef]
9. Wu, B.; Li, S.; Liu, Y.; Smedley, K.M. A New Hybrid Boosting Converter for

Renewable Energy Applications. *IEEE Trans. Power Electron.* **2016**, *31*, 1203–1215. [Google Scholar] [CrossRef]
10. Gorji, S.A.; Mostaan, A.; My, H.T.; Ektesabi, M. Non-isolated buck–boost dc–dc converter with quadratic voltage gain ratio. *IET Power Electron.* **2019**, *12*, 1425–1433. [Google Scholar] [CrossRef]
11. Diaz-Saldierna, L.; Morales-Saldaña, J.; Ortiz-Lopez, M. Switching regulator using a quadratic boost converter for wide DC conversion ratios. *IET Power Electron.* **2009**, *2*, 605–613. [Google Scholar] [CrossRef]
12. Starzyk, J.A.; Jan, Y.-W.; Qiu, F. A DC-DC charge pump design based on voltage doublers. *IEEE Trans. Circ. Syst. I Regul. Pap.* **2001**, *48*, 350–359. [Google Scholar] [CrossRef] [Green Version]
13. Luo, F.L.; Ye, H. Positive output multiple-lift push–pull switched capacitor Luo-converters. *IEEE Trans. Ind. Electron.* **2004**, *51*, 594–602. [Google Scholar] [CrossRef]
14. Lee, S.-W.; Do, H.-L. Quadratic Boost DC–DC Converter With High Voltage Gain and Reduced Voltage Stresses. *IEEE Trans. Power Electron.* **2018**, *34*, 2397–2404. [Google Scholar] [CrossRef]
15. Wai, R.-J.; Lin, C.-Y.; Duan, R.-Y. High-efficiency DC-DC converter with high voltage gain and reduced switch stress. *IEEE Trans. Ind. Electron.* **2007**, *54*, 354–364. [Google Scholar] [CrossRef]
16. Lee, J.; Liang, T.; Chen, J. Isolated coupled-inductor-integrated DC-DC converter with non-dissipative snubber for solar energy applications. *IEEE Trans. Ind. Electron.* **2014**, *61*, 3337–3348. [Google Scholar] [CrossRef]
17. Azizkandi, M.E.; Sedaghati, F.; Shayeghi, H.; Blaabjerg, F. A High Voltage Gain DC–DC Converter Based on Three Winding Coupled Inductor and Voltage Multiplier Cell. *IEEE Trans. Power Electron.* **2019**, *35*, 4558–4567. [Google Scholar] [CrossRef]
18. Duong, T.-D.; Nguyen, M.-K.; Tran, T.-T.; Lim, Y.-C.; Choi, J.-H. Transformerless High Step-Up DC-DC Converters with Switched-Capacitor Network. *Electronics* **2019**, *8*, 1420. [Google Scholar] [CrossRef] [Green Version]
19. Ahmad, J.; Zaid, M.; Sarwar, A.; Tariq, M.; Sarwer, Z. A New Transformerless Quadratic Boost Converter with High Voltage Gain. *Smart Sci.* **2020**, *8*, 1–21. [Google Scholar] [CrossRef]
20. Park, K.B.; Moon, G.W.; Youn, A.J. Non isolated high step-up boost converter integrated with sepic converter. *IEEE Trans. Power Electron.* **2010**, *25*, 2266–2275. [Google Scholar] [CrossRef]
21. Meraj, M.; Bhaskar, M.S.; Iqbal, A.; Al-Emadi, N.; Rahman, S. Interleaved Multilevel Boost Converter With Minimal Voltage Multiplier Components for High-Voltage Step-Up Applications. *IEEE Trans. Power Electron.* **2020**, *35*, 12816–12833. [Google Scholar] [CrossRef]
22. Zhu, B.; Chen, S.; Zhang, Y.; Huang, Y. An Interleaved Zero-Voltage Zero-Current Switching High Step-Up DC-DC Converter. *IEEE Access* **2021**, *9*, 5563–5572. [Google Scholar] [CrossRef]
23. Alzahrani, A.; Ferdowsi, M.; Shamsi, P. A Family of Scalable Non-Isolated Interleaved DC-DC Boost Converters with Voltage Multiplier Cells. *IEEE Access* **2019**, *7*, 11707–11721. [Google Scholar] [CrossRef]

ISSN: 2583-6129
Volume: 04 Issue: 04 | April – 2025
DOI: 10.55041/ISJEM03246
An International Scholarly || Multidisciplinary || Open Access || Indexing in all major Database & Metadata

24. Dwari, S.; Parsa, L. An Efficient High-Step-Up Interleaved DC–DC Converter with a Common Active Clamp. *IEEE Trans. Power Electron.* **2010**, *26*, 66–78. [**Google Scholar**] [**CrossRef**]